Silicon-Organic Hybrid (SOH) Devices for Nonlinear Optical Signal Processing

W. Freude,[1] J.-M. Brosi,[1] C. Koos,[1] P. Vorreau,[1] L. C. Andreani,[2] P. Dumon,[3] R. Baets,[3] B. Esembeson,[4] I. Biaggio,[4] T. Michinobu,[5] F. Diederich,[5] and J. Leuthold[1]
[1]*Institute of High-Frequency and Quantum Electronics, University of Karlsruhe, 76131 Karlsruhe, Germany*
[2]*Department of Physics "A. Volta", University of Pavia, 27100 Pavia, Italy*
[3]*Photonics Research Group, Ghent University – IMEC, B-9000 Gent, Belgium*
[4]*Department of Physics, Lehigh University, Bethlehem, PA 18015, USA*
[5]*Laboratorium für Organische Chemie, ETH Zürich, Hönggerberg, HCI, CH-8093 Zürich, Switzerland*
Tel: +49 721 608-2492, Fax: +49 721 608-9098, e-mail: w.freude@ihq.uka.de

ABSTRACT
Silicon-on-insulator (SOI) is a promising material system for dense on-chip integration of both silicon photonic and electronic devices. The high refractive index of silicon enables strong light confinement and compact low-loss devices at telecommunication wavelengths. In addition, on-chip nonlinear optical signal processing becomes feasible, because the third-order nonlinear susceptibility $\chi^{(3)}$ of silicon is about 200 times that of glass, and because the tight light confinement enhances the nonlinear response. However, for many applications it would be desirable to have even stronger nonlinearities, and to exploit second-order $\chi^{(2)}$-nonlinearities which are negligibly small in mono-crystalline silicon. On the other hand, many organic materials are highly nonlinear, but have only a low refractive index. Silicon-organic hybrid (SOH) systems combine the strengths of both materials resulting in extremely large effective nonlinearities.

We report on the design of a 100 Gbit/s / 1 V modulator based on an 80 µm long slow-light SOI photonic crystal slot waveguide filled with a $\chi^{(2)}$-nonlinear organic material. Further, we demonstrate demultiplexing of a 120 Gbit/s signal to 10 Gbit/s with four-wave mixing in a 6 mm long SOI slot waveguide, on which an organic highly $\chi^{(3)}$-nonlinear material was deposited with a molecular beam.

Keywords: silicon photonics, optical nonlinearities in organic materials, electro-optic effect, Kerr effect, photonic crystal waveguides, modulators, all-optical signal processing.

1. INTRODUCTION

Higher capacity in optical transmission systems requires faster optical signal processing [1]. Modulators and multiplexers are key in this context, and silicon photonics offers an advanced platform for robust, highly-integrated devices that are able to guide and confine near-infrared light strongly. However, in silicon the lowest-order optical nonlinearity is the third-order susceptibility ($\chi^{(3)}$, Kerr effect) [2], which in addition is influenced by two-photon absorption and free carrier generation. This impedes optical signal processing at high speed, and therefore requires measures to remove free carriers [3] [4].

On the other hand, organic materials with strong second-order ($\chi^{(2)}$, electro-optic effect) or third-order ($\chi^{(3)}$) nonlinearities are available, but they suffer from rather low refractive indices and are therefore not well suited for concentrating light to a small cross-section area. Combining the strengths of both systems — silicon-on-insulator (SOI) structures for confining the light to a small interaction region, and filling this region with a highly-nonlinear organic material — results in silicon-organic hybrid (SOH) devices with superior performance [4].

In the following, we report on the design and the properties of two SOH components:

- An ultra-compact SOH Mach-Zehnder (MZ) amplitude modulator [5], which is expected to have a modulation bandwidth of 78 GHz for transmitting data at 100 Gbit/s with a drive voltage of only 1 V. Our design combines the large field concentration of slot waveguides (WG), the high $\chi^{(2)}$-nonlinearity of organic materials, and the increased interaction time by a slow-light photonic crystal (PC) structure [6]. By careful design, chromatic dispersion can be eliminated in an optical bandwidth of 1 THz.
- An integrated SOH waveguide [7] with a $\chi^{(3)}$-nonlinearity of $\gamma = 10^5\,\mathrm{W^{-1}km^{-1}}$. A device with 6 mm length has been successfully tested [8] for its capability to demultiplex a 120 Gbit/s signal to 10 Gbit/s employing four-wave mixing (FWM). The optical mode is guided by a slotted waveguide and strongly confined to the slot. This interaction region is filled with a highly nonlinear organic material showing only little two-photon absorption (TPA).

2. MACH-ZEHNDER MODULATOR

The MZ modulator schematic is shown in Fig. 1(a). Phase modulators (PM) are inserted in both interferometer arms and driven in push-pull mode. Each PM consists of a slot PC-WG filled with a $\chi^{(2)}$-nonlinear organic material. The electric field is mainly confined to the slot, Fig. 1(b). The modulating voltage is applied to the PM electrodes and transferred to the slot region via conductive silicon slabs. In addition to the effect of strong field con-

978-1-4244-2625-6/08/$25.00 ©2008 IEEE

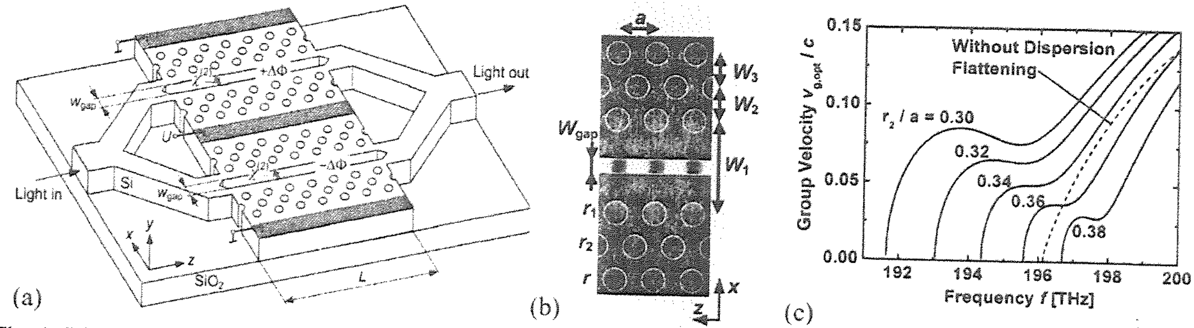

Fig. 1. SOH Mach-Zehnder modulator **(a)** Schematic. Y-branch (MMI coupler in reality) splits light in two arms. Phase modulators with narrow gap w_{gap} filled with $\chi^{(2)}$-nonlinear organic material inside a PC-WG designed for low group velocity to enhance nonlinear interaction. Silicon of the PC is doped. Electrodes (shaded) attached to supply modulating voltage U. **(b)** Dominant optical E-field. The gap is filled with organic material, and both, modulating voltage and optical field, are strongly confined to the gap. **(c)** Group velocity of slotted photonic crystal W1.25 WG. Region of constant low group velocity controlled with r_2. Parameters: $W_1 = 1.25\sqrt{3}\,a$, $W_2 = 0.65\sqrt{3}\,a$, $W_3 = 0.45\sqrt{3}\,a$, $r_1 = 0.25\,a$, $r = 0.3\,a$, silicon slab height 220 nm, gap width $W_{gap} = 150$ nm, PC period $a = 408$ nm. (– – – –): W1.4 WG without dispersion flattening of $v_{g,\,opt}$.

finement, the interaction in the PM sections is further enhanced by slowing down the optical group velocity $v_{g,\,opt}$, which allows reducing the modulator length L. To avoid distortions of optical pulses, the chromatic dispersion has been flattened in a 1 THz optical bandwidth, see Fig. 1(c). Without dispersion flattening (i. e., all PC holes have same radii), the group velocity changes strongly with optical frequency (Fig. 1(c), dashed line).

In Table 1, estimates of the MZ modulator bandwidth f_{3dB} and its associated length L are given by evaluating Eqs. (1)–(2) [5]. The estimates are for a fixed π-voltage U_π of the PM and a modulation amplitude $\hat{U} = U_\pi/4 = 1$ V. The electrical group velocity is $v_{g,el} \gg v_{g,\,opt}$, the refractive index of the organic material is

$$f_{3dB} = \frac{0.5\,v_{g,opt}}{L}\,\frac{1}{\left|1+v_{g,opt}/v_{g,el}\right|} \approx \frac{0.5\,v_{g,opt}}{L} \qquad (1)$$

$$U_\pi = \frac{c}{n_{org}^3 f_0}\,\frac{W_{gap}}{r_{33}}\,\frac{1}{\Gamma L} \propto \frac{W_{gap}}{r_{33}}\,\frac{v_{g,opt}}{L} \qquad (2)$$

Table 1
Characteristic Data for PC Slot Waveguide Modulator

R_2 / a	f_0 (THz)	$v_{g,opt}/c$	L (μm)	f_{3dB} (GHz)
0.38	197.5	3.2%	57	87
0.36	**196.5**	**4.0%**	**80**	**78**
0.34	195.8	5.2%	111	71
0.32	195.2	6.6%	158	61
0.30	194.6	7.9%	215	53

assumed to be $n_{org} = 1.6$, and its electro-optic coefficient is $r_{33} = 80$ pm/V. The quantity Γ stands for the electro-optic field interaction factor [5]. The data in Table 1 refer to the dispersion-flattened structures in Fig. 1(c). Out of these structures, one with a sufficiently flat dispersion at a realizable optical group velocity of 4 % of the vacuum speed of light was chosen, bold-face row in Table 1. A large modulation bandwidth of 78 GHz is predicted for a phase modulator length of 80 μm, allowing 100 Gbit/s transmission. The bandwidth f_{3dB} is limited by walk-off between optical and electrical signals, Eqs. (1)–(2), while electrical RC-effects do not play a role [5].

Signals from an external fibre may be effectively coupled to a conventional strip WG mode with coupling losses below 1 dB (see Ref. 19 in [5]). However, an efficient method is also needed to excite the slow-light mode within the PC slot WG. We propose a coupling structure which provides electrical isolation across the gap. It consists of two sections, which are schematically shown in Fig. 2(a), (b). Calculated transmission and reflection

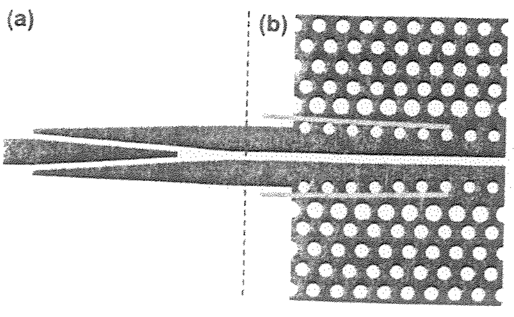

Fig. 2. Coupling transition from **(a)** strip-WG to slot-WG and to **(b)** PC WG. Transmission significantly increased by introducing a PC taper. W_1 of PC-WG slightly decreased from $1.45\sqrt{3}a$ to $1.25\sqrt{3}a$ over some lattice periods, overlaid tilted (green) lines. W_2 increased from $0.55\sqrt{3}a$ to $0.65\sqrt{3}a$. Width of strip-WG is 440 nm, gap width of slot-WG and PC-WG is 150 nm.

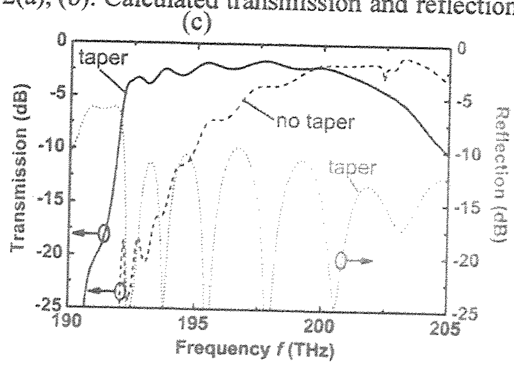

Fig. 3. Transmission and reflection for the transition from slot-WG to PC-WG and back to slot-WG, Fig. 2(b), with and without a PC taper. The introduction of the PC taper significantly enhances the transmission to a value better than −4 dB. The reflection is below −10dB.

curves are displayed in Fig. 3. The simulated structure comprises both the transition from a slot WG to a slow-light PC WG, Fig. 2(b), and the transition back to a slot WG. The transmission is better than –4dB including both tapers, while it drops below –20dB without tapers. The reflection stays below –10dB. For the transmission curve with tapers, residual Fabry-Perot fringes from reflections at the interfaces can be observed.

3. DEMULTIPLEXER WITH FOUR-WAVE MIXING

Four-wave mixing (FWM) in nonlinear waveguides [2] [9] can be used for demultiplexing OTDM signals. For fabricating a suitable waveguide, an organic material with large $\chi^{(3)}$-nonlinearity is deposited onto an SOI slot waveguide using a molecular beam, see the schematic in Fig. 4(a) and the focussed-ion beam image in Fig. 4(c). To maximize the nonlinearity we need to optimize the nonlinear parameter $\gamma = n_2\, k_0 / A^{(3)}{}_{\mathrm{eff}}$. In this relation, $A^{(3)}{}_{\mathrm{eff}}$ is the effective area of nonlinear interaction, which depends on the waveguide geometry, k_0 denotes the free-space wave number, and n_2 is the intensity-related nonlinear index coefficient.

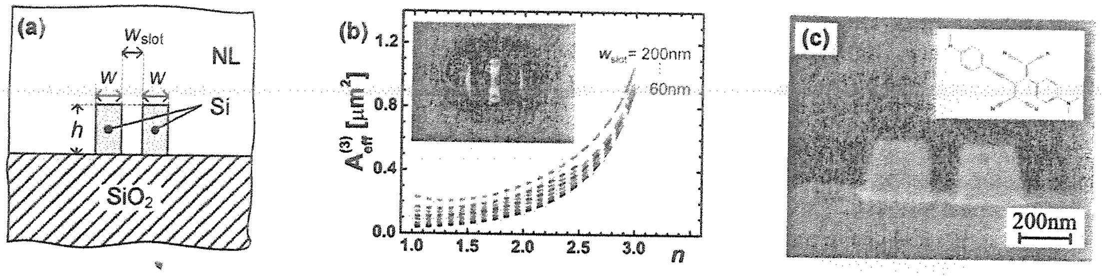

Fig. 4. (a) Cross section of slot waveguide with two silicon (Si) ribs on a silicon dioxide buffer layer (SiO_2), covered by a nonlinear material (NL). **(b)** Effective area for nonlinear interaction as a function of the linear refractive index n_{NL} of the nonlinear cover material. Strip width w and waveguide height h optimized for fixed slot widths w_{slot}. *Inset:* Field plot of the dominant electric field component (E_x parallel to substrate plane) for a slot width $w_{slot} = 100$ nm and $n_{NL} = 1.5$. **(c)** Cross section of fabricated slot waveguide functionalized with organic film. *Inset:* Molecular structure of nonlinear organic material. — SOI templates fabricated on 200 nm CMOS line using 193 nm DUV lithography on an ASML PAS5500/1100 stepper and Cl-based reactive ion etching [12]. Thickness of SOI device layer (waveguide height) $h = 220$ nm, buried oxide thickness 2 µm. Strip (slot) widths w (w_{slot}) range from 160 nm to 220 nm (150 nm to 250 nm). Waveguides functionalized by molecular beam deposition of an amorphous organic film with 950 nm thickness. The film consists of DDMEBT (2-[4-(Dimethylamino)phenyl]-3-{[4-(dimethylamino)phenyl]ethynyl}buta-1,3-diene-1,1,4,4-tetracarbonitrile). The molecules are described in more detail as derivative 2 in [13]. The refractive index of the organic film is $n = 1.8$ at a wavelength of 1.5 µm, and its nonlinear index coefficient amounts to $n_2 \approx 2 \times 10^{-17}\,\mathrm{m^2/W}$; this is 1 000 times larger than for fused silica.

We optimize the waveguide geometry for maximum confinement of the optical mode in the slot. By varying the rib width w and the height h, and by choosing realizable slot widths of $w_{slot} \geq 60$ nm, the area $A^{(3)}{}_{\mathrm{eff}}$ can become significantly smaller than 0.1 µm², Fig. 4(b). The field intensity has been further enhanced ([7], see Fig. 4(b)) by choosing an organic slot material with the smallest refractive index available. This results in a four-fold field enhancement due to the discontinuity of the normal electric field component at the interface of silicon (refractive index 3.48) and the organic material (refractive index 1.8). Fibre-chip coupling losses amount to $a_{cp} = 3.8$ dB per facet, and the propagation loss is 2.3 dB/mm ($\alpha = 0.53\ \mathrm{mm^{-1}}$) at 1550 nm.

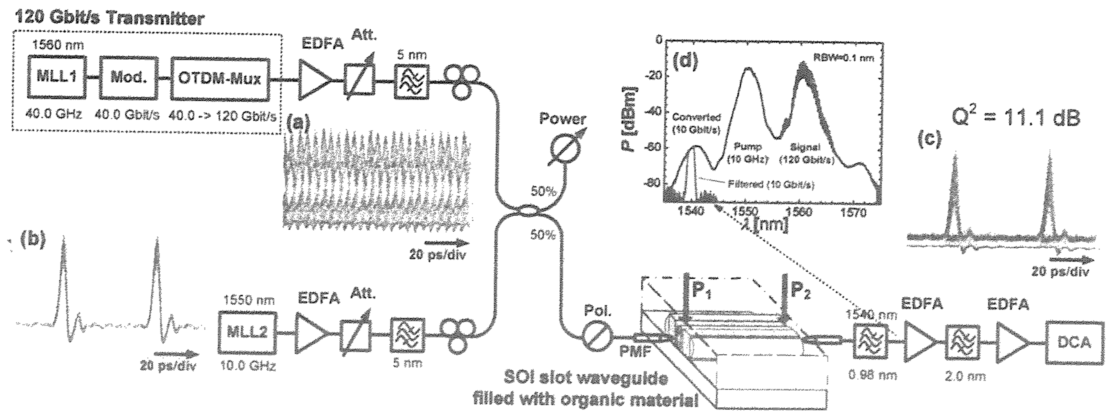

Fig. 5. SOH FWM demultiplexer. Slot waveguide filled with organic material. **(a)** 120 Gbit/s signal **(b)** 10 GHz pump **(c)** Demultiplexed 10 Gbit/s signal **(d)** Spectrum at the output of the DUT and after bandpass-filtering. — MLL1, MLL2 = mode-locked lasers, Mod = data modulator, OTDM-Mux = optical time-division multiplexer, EDFA = erbium-doped fibre amplifier, Att = attenuator, Power = power meter, Pol = polarizer, PMF = polarization maintaining fibre, DUT = device under test, DCA = digital communication analyzer

The effective nonlinear interaction length is $L_{\text{eff}} = [1 - \exp(-\alpha L)] / \alpha = 1.89$ mm for the 6 mm long waveguide. We measured the conversion efficiency $\eta = \exp(-\alpha L)\,(\gamma P_p L_{\text{eff}})^2$ of partially degenerate FWM with continuous-wave pump and signal, where P_p denotes the on-chip pump power at the beginning of the waveguide. A record nonlinear parameter $\gamma = 10^5\ \text{W}^{-1}\text{km}^{-1}$ was inferred, much larger than with holey fibres (1 860 $\text{W}^{-1}\text{km}^{-1}$) [10] and larger than with chalcogenide (68 000 $\text{W}^{-1}\text{km}^{-1}$) fibres [11].

We performed all-optical demultiplexing of a 120 Gbit/s signal down to a 10 Gbit/s data stream. The experimental setup together with the eye diagrams is depicted in Fig. 5. For the data (pump) we used mode-locked fibre lasers operating at repetition rates of 40 GHz (10 GHz) and emitting pulses of approximately 3 ps FWHM. The 120 Gbit/s data were generated by modulating the 40 GHz pulse train with a pseudo-random bit sequence of length $2^{31} - 1$, and by subsequent time multiplexing. The output signal was bandpass-filtered at the converted wavelength, amplified, and the resulting eye diagram was recorded with a digital communication analyzer. By varying the delay between pump and signal, different tributaries could be demultiplexed. From the eye diagram, a Q-factor of $Q^2 = 11.1$ dB was measured for an on-chip pump power of 15.6 dBm (36 mW).

4. CONCLUSIONS

Two devices demonstrate the potential of silicon-organic hybrid (SOH) photonics: First, we report on the design of an SOH MZ modulator with 1 V drive voltage based on a 80 µm long slow-light photonic crystal line-defect slot waveguide filled with a $\chi^{(2)}$-nonlinear organic material. In an optical bandwidth of 1 THz we predict a transmission at 100 Gbit/s. Second, we functionalize a 6 mm long SOH slot waveguide with a $\chi^{(3)}$-nonlinear organic cladding resulting in a record nonlinearity of $\gamma = 10^5\ \text{W}^{-1}\text{km}^{-1}$. As an application, we demultiplex a 120 Gbit/s data stream to 10 Gbit/s employing partially degenerate FWM with 15.6 dBm on-chip pump power.

ACKNOWLEDGEMENTS

This work was supported by the Deutsche Forschungsgemeinschaft (DFG) in the Priority Program SP 1113 "Photonic Crystals", by the DFG Center for Functional Nanostructures (CFN), by the Initiative of Excellence of the University of Karlsruhe, by the European project TRIUMPH (grant IST-027638 STP), and by the Deutsche Telekom Stiftung. We acknowledge technological support by the European Network of Excellence ePIXnet (silicon photonics platform) and by ASML Netherlands B.V., and we acknowledge equipment loan from Siemens Portugal and from Optoelectronics Research Centre (ORC) in Southampton, UK. I. B. and B. E. acknowledge partial support from the Commonwealth of Pennsylvania, Ben Franklin Technology Development Authority. F. D. and T. M. acknowledge support from the ETH research council.

REFERENCES

[1] L. Liao, A. Liu, D. Rubin, J. Basak, Y. Chetrit, H. Nguyen, R. Cohen, N. Izhaky, M. Paniccia: 40 Gbit/s silicon optical modulator for high-speed applications, *Electron. Lett.*, vol. 43, 20072253, Oct. 2007.

[2] Y.-H. Kuo, H. Rong, V. Sih, S. Xu, M. Paniccia, O. Cohen: Demonstration of wavelength conversion at 40 Gb/s data rate in silicon waveguides, *Opt. Express*, vol. 14, pp. 11721-11726, Nov. 2006.

[3] H. Rong, A. Liu, R. Jones, O. Cohen, D. Hak, R. Nicolaescu, A. Fang, M. Paniccia: An all-silicon Raman laser, *Nature*, vol. 433, pp. 292-294, Jan. 2005.

[4] M. Hochberg, T. Baehr-Jones, G. Wang, J. Huang, P. Sullivan, L. Dalton, A. Scherer: Towards a millivolt optical modulator with nano-slot waveguides, *Opt. Express*, vol. 15, pp. 8401-8410, June 2007.

[5] J.-M. Brosi, C. Koos, L. C. Andreani, M. Waldow, J. Leuthold, W. Freude: High-speed low-voltage electro-optic modulator with a polymer-infiltrated silicon photonic crystal waveguide, *Opt. Express*, vol. 16, pp. 4177–4191, March 2008.

[6] L. Gu, W. Jiang, X. Chen, L. Wang, R. T. Chen: High speed silicon photonic crystal waveguide modulator for low voltage operation, *Appl. Phys. Lett.*, vol. 90, 071105, Feb. 2007.

[7] C. Koos, L. Jacome, C. Poulton, J. Leuthold, W. Freude: Nonlinear silicon-on-insulator waveguides for all-optical signal processing, *Opt. Express*, vol. 15, pp. 5976-5990, May 2007.

[8] C. Koos, P. Vorreau, P. Dumon, R. Baets, B. Esembeson, I. Biaggio, T. Michinobu, F. Diederich, W. Freude, J. Leuthold: Highly-nonlinear silicon photonics slot waveguide, *Technical Digest Optical Fiber Commun. Conf.* (OFC 2008), San Diego (CA), USA, Feb. 24–28, 2008. Postdeadline Paper PDP25.

[9] R. Salem, M. A. Foster, A. C. Turner, D. F. Geraghty, M. Lipson, A. L. Gaeta: Signal regeneration using low-power four-wave mixing on silicon chip, *Nature Photonics*, vol. 2, pp. 35-38, Jan. 2008

[10] J. Y. Y. Leong, P. Petropoulos, S. Asimakis, H. Ebendorff-Heidepriem, R. C. Moore, K. Frampton, V. Finazzi, X. Feng, J. H. V. Price, T. M. Monro, D. J. Richardson: A lead silicate holey fiber with $\gamma = 1\,860\ \text{W}^{-1}\text{km}^{-1}$ at 1550 nm, *Technical Digest Optical Fiber Commun. Conf.* (OFC 2005), Anaheim (CA), USA, March 6–11, 2005. Postdeadline Paper PDP22.

[11] E. C. Mägi, L. B. Fu, H. C. Nguyen, M. R. E. Lamont, D. I. Yeom, B. J. Eggleton: Enhanced Kerr nonlinearity in sub-wavelength diameter As_2Se_3 chalcogenide fiber tapers, *Optics Express*, vol. 15, pp. 10324-10329, Aug. 2007.

[12] W. Bogaerts, P. Dumon, D. Van Thourhout, D. Taillaert, P. Jaenen, J. Wouters, S. Beckx, R. Baets: Compact wavelength-selective functions in silicon-on-insulator photonic wires, *IEEE J. Sel. Topics Quantum Electron.*, vol. 12, pp. 1394-1401, Nov. 2006.

[13] T. Michinobu, J. C. May, J. H. Lim, C. Boudon, J.-P. Gisselbrecht, P. Seiler, M. Gross, I. Biaggio, F. Diederich: A new class of organic donor–acceptor molecules with large third-order optical nonlinearities, *Chem. Commun.*, vol. 36, pp. 737-739, Jan. 2005.

ICTON 2008

10th Anniversary International Conference on Transparent Optical Networks

collocated with:

ESPC 7th European Symposium on Photonic Crystals
WAOR 7th Workshop on All-Optical Routing
GOWN 5th Global Optical & Wireless Networking Seminar
RONEXT 4th Workshop on Reliability Issues in Next Generation Optical Networks
PICAW 4th Photonic Integrated Components & Applications Workshop
NAON 3rd COST 288 Nanophotonics for All-Optical Networking Workshop

and special sessions:

MPM – Microresonators and Photonic Molecules: trapping, harnessing and releasing light
Industrial
Novel Glasses for photonic devices
Broadband Access: making use of optical transparency for user access
MARS – Market in Telecommunications

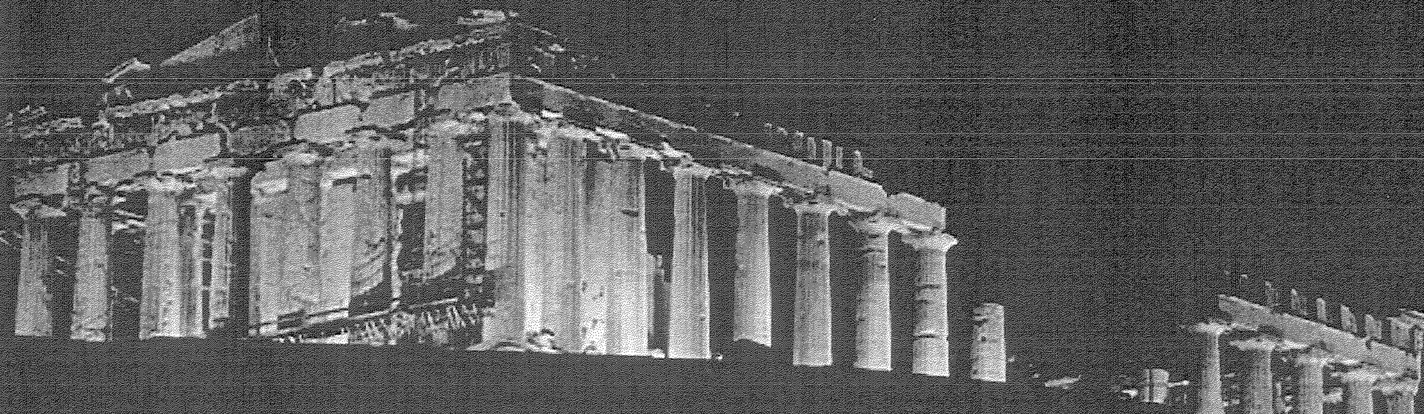

Volume 2

contains: ESPC, NAON, MARS

Athens, Greece, June 22 - 26, 2008

IEEE
Athens Information Technology
Instytut Łączności
IEEE LEOS THE SOCIETY FOR PHOTONICS
cost
INTRACOM TELECOM
grnet Networking Research and Education
LEOS Poland Chapter

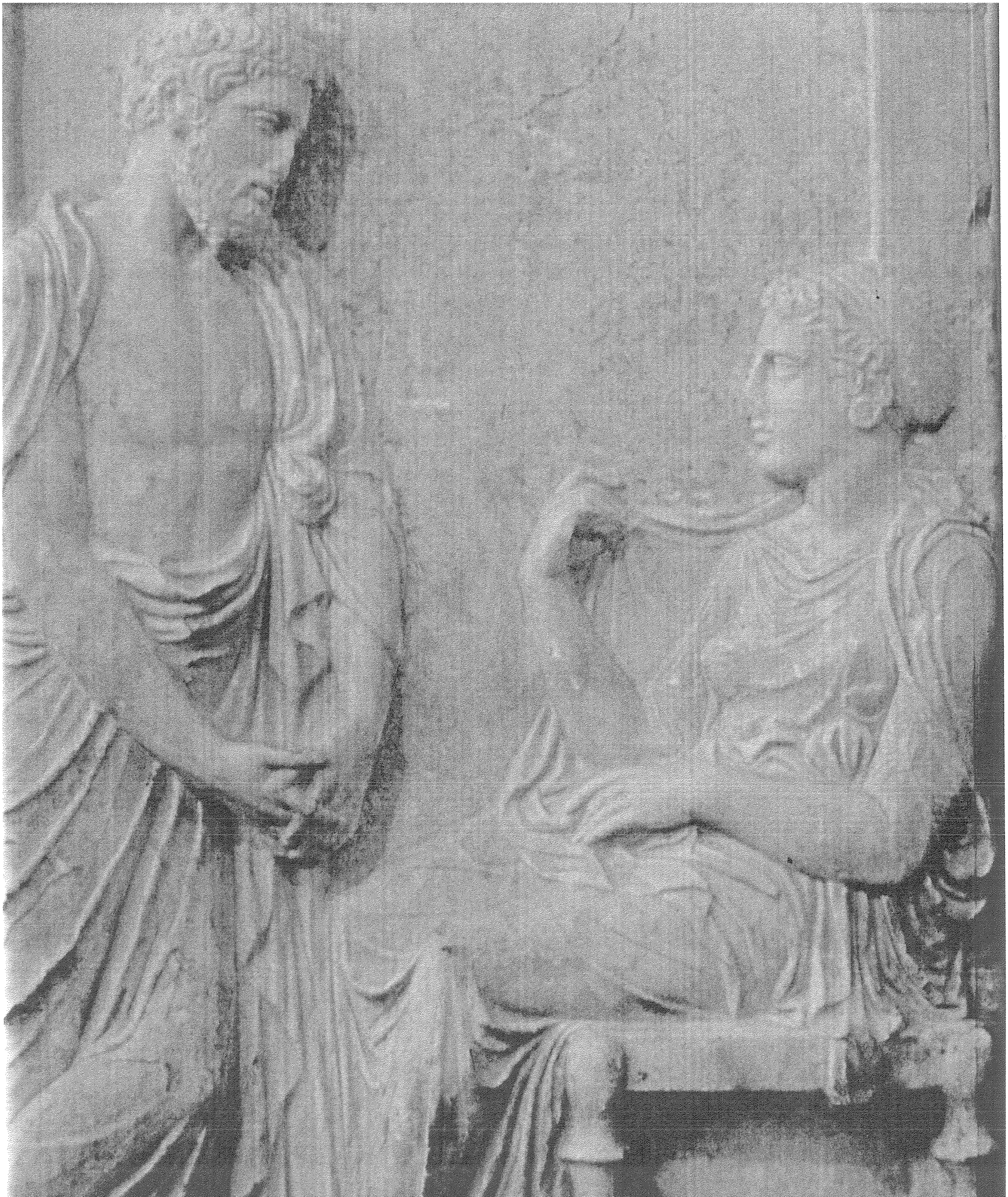

ISBN 978-1-4244-2625-6